

THERMAL SHOCK BEHAVIORS OF MgAlON AND MgAlON-BN COMPOSITE REFRACTORIES

Zuotai Zhang & Xidong Wang

Peking University, P. R. China

Zhang & Wenchao Li

University of Science and Technology, P. R. China

Seshadri Seetharaman

Royal Institute of Technology, Sweden

ABSTRACT

Thermal shock parameters (R , R''' and R'''') have been evaluated using three point bending strength and Young's modulus values for magnesium aluminum oxynitride-boron nitride (MgAlON-BN) composites. The calculation indicated that thermal shock resistance of MgAlON was improved by BN addition. The single thermal shock testing was carried out by means of quenching the specimen from high temperatures (ΔT in the range 400-1500°C). The damage introduced by thermal shock was characterized by the degradation of three point bending strength. The experimental results indicated that MgAlON-15vol%BN composite showed a better resistance to thermal shock than that of MgAlON, which showed the similar pattern with the calculated R''' and R'''' parameters. The SEM results showed that there were some linking cracks on the surface of MgAlON as well as on cross section, however, no obvious cracks were observed for MgAlON-15vol%BN composites in the same condition.

INTRODUCTION

Magnesium aluminium oxynitride, viz. MgAlON, has been referred to as a premium candidate for high performance refractories and high temperature structural materials under extreme working conditions because of its favorable combination of mechanical (hardness) and chemical properties [1, 2]. A number of investigations have shown that graphite refractories incorporating some MgAlON could improve the resistance to slag and steel corrosion [3, 4]. Hexagonal boron nitride (h-BN) with the structure similar to graphite shows excellent corrosion and thermal shock resistance, good mechanical tolerance and machinability. In fact, Si_3N_4 -BN [5], Sialon-BN [6] composites, have already been used as special refractory nozzles, tubes, break rings for the continuous casting of steel, etc. However, the decomposition of Si_3N_4 and Sialon by dissolution of silicon into molten steel restricted their wide application. In earlier papers, the present authors combined MgAlON and BN to obtain the MgAlON-BN composites [7, 8], which is expected to be used as high performance refractory or advanced instead of Sialon-BN and Si_3N_4 -BN. The physical properties, machinability [7, 8], wettability [9, 10] and thermal conductivity/diffusivity [9, 10] have been studied, indicating that MgAlON-15vol%BN composite shows the excellent properties as refractories. Thermal shock property is another important parameter for refractories or high properties of ceramics. To the best knowledge of present authors, no systemic study of thermal shock has been carried out so far. The present paper is thus motivated.

In the present paper, the thermal shock behavior of sintered MgAlON and MgAlON-15vol%BN composites were investigated using water quenching method. Thermal shock parameters were calculated to examine the properties of the composites. On the basis of these calculations, the damage introduced by single thermal shock was characterized by degradation of strength in three-point bending method. The surface morphology and cross sections of the tested samples after thermal shock experiment were also investigated.

THERMAL SHOCK PARAMETER

A number of thermal shock parameters have been defined over the past decades [11, 12]. In general, two different approaches are adopted to derive the thermal shock parameters. The first approach is based on a fracture resistance consideration in which thermoelastic theories are used and the attention is focused on the initiation of fracture because of the thermal stresses. The R , R' and R'' parameters are derived as the following equations,

$$R = \frac{\sigma_f (1 - \nu)}{E\alpha} \quad (1)$$

$$R' = \frac{\sigma_f (1 - \nu)k}{E\alpha} \quad (2)$$

$$\text{and } R'' = \frac{\sigma_f (1 - \nu)\Phi}{E\alpha} \quad (3)$$

where σ_f is the three point bending strength, E is the Young's modulus, α is the thermal expansion coefficient, ν is the Poisson's ratio, k is the thermal conductivity, and Φ is a stress reduction term. The parameter R is applicable for the case of an instantaneous change in surface temperature under conditions of rapid heat transfer. R' is for a relatively slow heat transfer, and R'' is for a constant heating or cooling rate.

The second approach to determine the thermal shock resistance of materials is focused on the crack propagation and the resulting changes in the physical properties of the material. In this case, two parameters for damage resistance R''' and R'''' are defined by Haselman as following [13, 14],

$$R''' = \frac{E}{\sigma_f^2 (1 - \nu)} \quad (4)$$

$$R'''' = \frac{E \gamma_{wof}}{\sigma_f^2 (1 - \nu)} \quad (5)$$

where γ_{wof} is the effective surface energy or work of fracture per unit projected area of fracture face. The R''' parameter gives information about the minimum in the elastic energy at fracture available for crack propagation, and the R'''' parameter is the minimum in the extent of crack propagation on initiation of thermal stress fracture. For typical refractory materials, the initial strength may be low, but may have a significant resistance to crack propagation or extension caused by thermal shock. Thus, it is necessary to predict the thermal shock durability by calculating R''' and R'''' for refractories [15, 16].

EXPERIMENTAL PROCEDURES

Materials Preparation

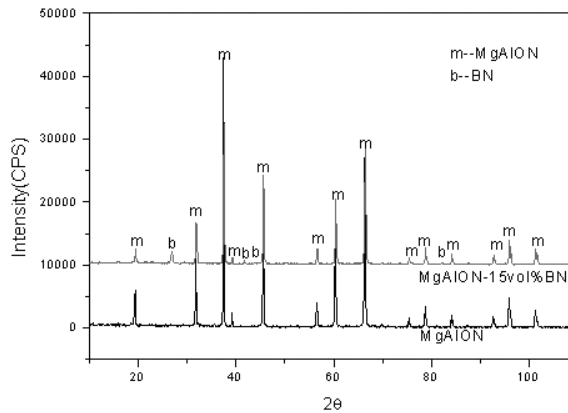


Figure 1: XRD patterns examined on the crushed powders with pure MgAlON and an addition of 15 vol% h-BN

The materials used in this study were fabricated using hot-pressing technique. The experimental procedures used to manufacture these materials have been described in detail elsewhere [7, 8], and is briefly outlined here. Appropriate amounts of the fine powders of Al_2O_3 , AlN, MgO and BN were mixed by ball milling in ethanol medium for 24 hours to prepare MgAlON and MgAlON-BN composites. The mixtures obtained this way were placed in a graphite mould covered with boron nitride coating and sintered at 2073 K, at 20 MPa, in argon gas atmosphere for 2 hours. The X-ray diffraction (XRD) results

confirmed the formation of pure MgAlON and MgAlON-BN composites, no impurities or amorphous phases were observed. Some XRD results are shown in Figure 1. The samples were cut, ground and polished into $3 \times 4 \times 40 \text{ mm}^3$ strips for thermal shock experiments.

Thermal Shock Experiments

Thermal shock experiments were performed in a vertical tube furnace in argon atmosphere. Specimens were held in the furnace for 30 minutes to allow for temperature equilibration at different temperatures followed by dropping them into a container of water at $15 \pm 5^\circ\text{C}$. Tests were carried out in the temperature range of 400°C to 1500°C . The samples after thermal shock experiments were cleaned with acetone, and then dried at 100°C for 5 hours. The strength of the quenched samples was determined using three point bending method.

Mechanical Properties Measurements

The retained strength and Young's Modulus of the specimens before and after the water quenching were measured using a three point bending method. The standard equations for the strength (σ_f) [17] and Young's Modulus (E) [18] of a bar in three point bending method can be described as follows,

$$\sigma_f = \frac{3}{2} \times \frac{PL}{bw^2} \quad (6)$$

$$E = \frac{L^3 a}{4bw^3} \quad (7)$$

where P is the load at fracture, L is the length of support span, b is the specimen width, w is the specimen thickness, a is the slope of the tangent of the initial straight-line portion of the load-deflection curve corrected for machine stiffness. Five specimens were normally tested to obtain a mean value.

Work of fracture (γ_{wof}) were calculated from load-deflection curves obtained from notched bars deformed in three-point bend, by measuring the area (U) under the load-deflection curve. γ_{wof} is given by the following equations [19, 20]:

$$\gamma_{wof} = \frac{U}{2b(w - c)} \quad (8)$$

where U is the area under the load-deflection curve, c is the notch depth.

Microstructure Analysis

The crystalline phases of the hot-pressed samples identified by XRD measurements were carried out in air with a flow rate of $10 \text{ cm}^3/\text{min}$ (STP) on a M21X-SRA X-ray diffractometer, manufactured by MAC Science Co. Ltd, Japan, equipped with graphite crystal diffracted-beam monochromator. The accelerating voltage and current were 40 kV and 300 mA respectively. Operating parameters involved were the following: receiving slit = 0.15 mm, divergence slit = 0.1° , scatter slit = 0.1° . Graphite crystal monochromator was employed. Intensities were collected by 2θ scanning. Specimens for transmission electron

microscope (TEM) studies before the thermal shock experiments were prepared by cutting thin sections perpendicular to hot-pressing direction from the hot-pressed discs. A section of the specimen was then mechanically polished to a thickness of less than 30 μm followed by on milling using a Gatan-600 ion beam thinner at a voltage of 4 kV and perforated. Finally, the ultra-thin plate was sputtered with amorphous carbon to the thickness of about several decades of nanometers. Scanning electron microscope (SEM) was used to analyze the surface and fracture section of specimens after thermal shock experiments. Gold was sputtered onto the sections as well as surface of specimen. Element analysis was performed on a JSM-6400 microscope equipped with an energy dispersive spectroscope (EDS) system.

RESULTS

Phase Identification and Mechanical Properties

Figure 1 shows XRD patterns of pure MgAlON and MgAlON-15vol%BN composites synthesized by hot pressing technique at 1800°C under N_2 atmosphere for 2 h with the hot-pressing pressure 20 MPa. The spectra identified that the main phase was MgAlON, the second was h-BN phase. No impurities were found. In view of the importance of the strength and Young's modulus for the calculation of the thermal shock parameters (R , R''' and R''''), it was necessary to measure the strength and Young's modulus values. The strength and modulus followed the same trend, i.e., decreased with increasing of BN content. Figure 2 presents the results.

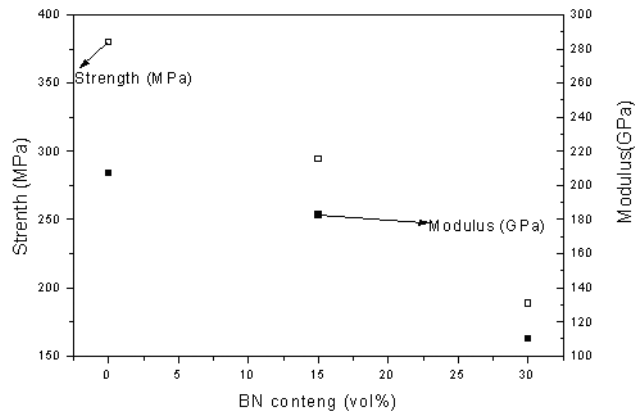


Figure 2: Strength and modulus as functions of BN contents

Thermal Shock Parameters

Figure 3 shows the R parameter as a function of BN volume fraction. Initially, the R parameter decreased slightly followed by an increase with increasing of BN content. It should be pointed out that the flake BN demonstrates anisotropic properties. Thermal expansion coefficient of BN perpendicular to c axis ($\alpha_{\perp} = 1 \times 10^{-6} \text{K}^{-1}$) was used during calculation of R parameter.

Figure 4 gives the R''' parameter as a function of BN volume fraction. As can be seen, the R''' parameter increased with increasing of BN content. Work of fracture (γ_{wof}) values calculated from the areas under the load-deflection curve in the present work was shown in Figure 5. There was a general marked decrease in work of fracture. In general, the R''''

parameter is more significant than R''' parameter because of R'''' parameter calculation combined with γ_{wof} . As shown in Figure 6, the R'''' parameter also increased with BN addition in the present calculation, and exhibited a similar pattern in terms of BN addition in close analogy to the R''' parameter.

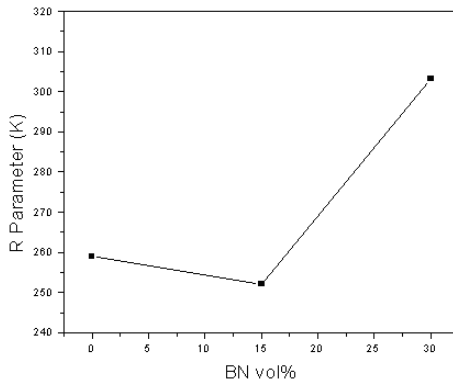


Figure 3: R parameter versus BN content

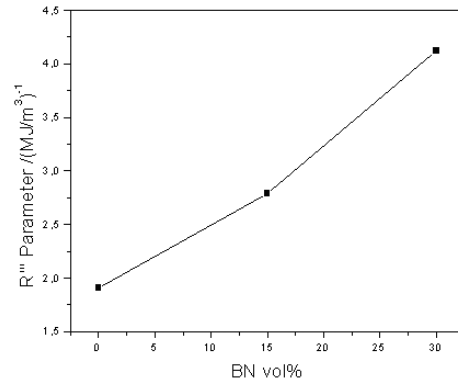
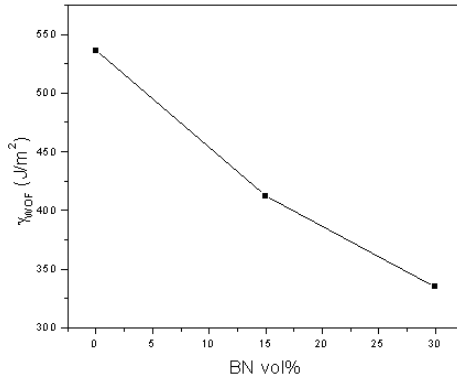
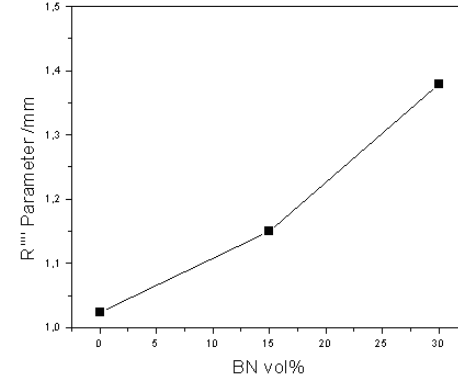
Figure 4: R''' parameter versus BN content

Figure 5: Work of fracture versus BN content

Figure 6: R'''' parameter versus BN content

Retained Strength after Thermal Shock

Figure 7 shows the effect of single thermal shock on the strength of MgAlON and MgAlON-15vol%BN composites. It could be separated into two stages with increasing of thermal shock temperature difference. Initially, the strength of MgAlON and MgAlON-15vol%BN composites remained constant for a substantial temperature range. The second stage is corresponding to the strength degradation. Figure 8 gives the fraction of retained strength as a function of temperature differences. As can be seen, the fraction of retained strengths are 37% and 53% for MgAlON and MgAlON-15vol% composites respectively after thermal shock temperature difference 1500°C. This indicated that MgAlON-15vol%BN composites show a better thermal shock resistance than that in MgAlON.

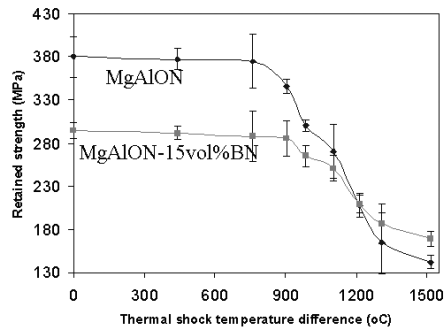


Figure 7: Retained strength versus thermal shock temperature difference, for MgAlON and MgAlON-15vol%BN composites

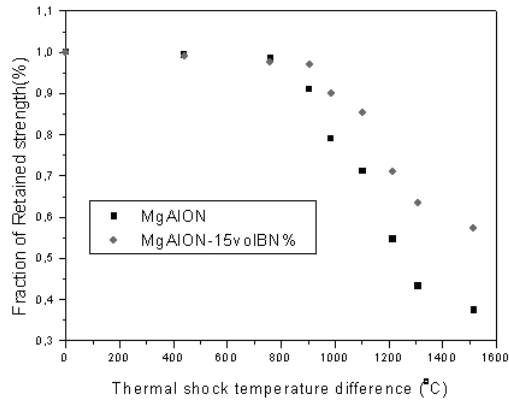


Figure 8: Fraction of retained strength versus thermal shock temperature difference, for MgAlON and MgAlON-15vol%BN

SEM Morphology

Figure 9 gives the surface morphology for MgAlON and MgAlON-15vol%BN composites after thermal shock temperature difference 440 and 1500°C, respectively. No obvious cracks were found after thermal shock temperature difference 440°C for both composites. There were some obvious linking cracks on the surface and cross sections for MgAlON (Figure 9(a) and (b)), but no obvious cracks were found for the MgAlON-15vol%BN composite after thermal shock temperature difference 1500°C. It should be pointed out that the samples were oxidized after thermal shock temperature difference 1500°C, as can be seen from Figure 9(c) and (d). It is reasonable to assume that the oxidation has no effect on the obtained results due to the oxidation occurring on the surface.

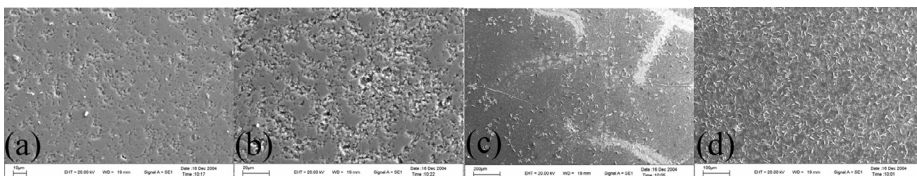


Figure 9: Surfaces morphology for (a)(c)MgAlON and (b)(d)MgAlON-15vol%BN samples after thermal shock experiment from $\Delta T_c = 440^\circ\text{C}$ and 1500°C

DISCUSSION

H-BN exhibits considerable anisotropy of many of its properties such as thermal expansion, thermal conductivity as well as thermal diffusivity and demonstrates low Young's modulus, density properties and non-reactive nature. Thus, the physical properties such as density, strength, Young's modulus of BN-based composites decrease and the porosity of composites increase with increasing of BN addition. The previous work demonstrated that the interwoven microstructure was formed when the BN addition was lower than 20vol%, and further addition of BN led to discontinuous microstructure of composites [7, 8].

In cooling from the fabrication temperature, a particle with a larger thermal expansion coefficient than the matrix induces tangential compressive stresses and radial tensile stresses. Alternatively, particles with a smaller thermal expansion coefficient create tangential tensile stresses and radial compressive stresses [21]. For the present case, the thermal expansion coefficients of BN in different directions are $\alpha_{\perp}=1\times 10^{-6}\text{K}^{-1}$ and $\alpha_{//}=7.51\times 10^{-6}\text{K}^{-1}$, respectively. The thermal expansion coefficient of MgAlON is $\alpha=5.31\times 10^{-6}\text{K}^{-1}$. At the MgAlON/BN interface parallel to the hexagonal axis of BN, the radial compressive stress may clamp the interface, forming some microcracks, whereas at MgAlON/BN interface perpendicular to the hexagonal axis of BN, the radial tensile stress may also form some microcracks [7, 8]. Thermal residual stresses induced by thermal expansion mismatch can be calculated using the Selsing equation [22].

$$P^{res} = \frac{2(\alpha_m - \alpha_p)\Delta TE_m}{(1 + \nu_m) + 2\beta(1 - 2\nu_p)} \quad (9)$$

where E_m , E_p , ν_m , ν_p , α_m and α_p are Young's modulus, Poisson's ratios and thermal expansion coefficients of the matrix and particle. ΔT is the temperature difference between the fabrication temperature ignoring plastic transform and room temperature. Thus, thermal stresses on the interfaces between MgAlON/BN (perpendicular) and MgAlON/BN(parallel) were calculated, and the values were 364.6 MPa and -176.7 MPa, respectively. The anisotropy of BN also can induce the thermal stresses, and these could be described as follows [22],

$$\sigma_z = \frac{E\Delta T}{(1 - \nu^2)} [(\alpha_{//} - \alpha) - \nu(\alpha_{\perp} - \alpha)] \quad (10)$$

where E and α are the mean Young's modulus and thermal expansion coefficient of composite materials respectively. The thermal stresses can thus be calculated by Equation(10) and the value was -417.4 MPa. It should be pointed out that overall residual stresses were not the sum of above three calculated values. These can be explained by the following reasons: i) BN particles are distributed on the grain boundaries of MgAlON. This increases the randomness of orientation of BN particles, and consequently changes the anisotropy of BN with respect to thermal expansion coefficient; ii) It is impossible to fabricate the full dense composites, the porosity in composites can absorb some elastic energy and consequently results in the decrease of the residual stresses; iii) The change of physical parameters with thermal shock temperature difference, such as Young's modulus, Poisson's ratio and thermal expansion coefficient were ignored. Some microcracks were observed with several micrometers length in the composite materials induced by the thermal stress [7, 8]. It's far lower however than the calculated values, as shown in Table 1. This indicated that the microcracks have a small influence on the strength of composites, but it would have much effect on the thermal shock properties of composites.

The microcracks had the more negative effect on strength than Young's modulus with the 15vol% BN addition, as can be seen from Figure 2. This resulted in the slightly decrease of R parameter. 30vol%BN addition however led to the discontinuous microstructure with MgAlON [7, 8]. BN flakes were distributed on the grain boundaries in this case instead of interwoven microstructure [7, 8]. Furthermore, the mean thermal expansion coefficient decreased (Table 1), and consequently led to the increase of R parameter. Since the MgAlON-BN composite materials are not always resistant to fracture initiation by the thermal stress, the R''' and R'''' parameters must be taken into account in characterizing further thermal shock damage [15]. The R''' expresses the ability of a material to resist crack propagation and further damage and loss of strength on thermal shocking. The trends in the R''' parameter are consistent with the measurements of thermal shock damage caused by water quenching.

The sintering of the MgAlON-BN composite seems to be predominantly promoted by forming of MgAlON particles due to the non-reactive nature of BN and that the BN particles might prevent contact between MgAlON particles and accordingly restrain the sintering of the composite [9, 10]. Thus, it can be concluded that the grain boundary energy between MgAlON grains is higher than that between MgAlON and BN grains. This resulted in the decrease of work of fracture, and can be verified by the SEM analysis. The fracture surface of pure MgAlON showed part of intergranular cracks [9, 19]. Further addition of BN however lead to the occurrence of transgranular fracture [7, 8]. It appears that intergranular cracks require much more energy for fracture. Therefore, the lower values of γ_{WOF} are associated with the lower grain boundary energy and the occurrence of more intergranular fracture instead of transgranular fracture.

Table 1: Parameters affecting thermal shock durability, ΔT_c for MgAlON, MgAlON-BN and BN ceramics

	MgAlON	-15vol%BN	-30vol%BN	h-BN
$E(GPa)$	207	182.65	110.01	65
$\gamma_{wof}(J \cdot m^{-2})$	535.95±11.81	412.20±23	334.80±15.37	---
$\alpha(K^{-1})$	5.31×10 ⁻⁶	^a 4.814×10 ⁻⁶	^a 4.275×10 ⁻⁶	1.0×10 ⁻⁶
ν	0.25	^a 0.24	^a 0.24	0.23
$\sigma(MPa)$	379.68	294.4	168.59	28
$K_{IC}(MPa \cdot m^{-1/2})$	3.23	3.64	2.26	---
$C(\mu m)$	32	67	63	---

^a Calculated using *Composite law* based on the values of each monolith, MgAlON and BN

^o Calculated using equ. $K_{IC} = (2E\gamma_i)^{1/2} = (\sigma Y C)^{1/2}$, where $Y=1.5$

E: Young's modulus, γ_{wof} work of fracture, α thermal expansion coefficient, ν Poisson's ratio, K_{IC} fracture toughness, C critical crack length

CONCLUSIONS

The thermal shock behaviour of MgAlON-BN composite materials were investigated in the present paper by water quenching experiments. The results showed that the strength of composite materials remain constant for a substantial temperature range followed by a strength degradation gradually. The fraction of retained strength was improved from 37% to 53% at the thermal temperature difference 1500°C. The experimental results showed the same trends with the calculation of R''' and R'''' . These were contributed to thermal stresses induced by thermal mismatch between MgAlON and BN. Furthermore, BN with non-reactive nature led to the increase of porosity. The SEM results indicated that the

surface and cross sections for MgAlON after thermal shock experiments had some linking cracks after thermal shock temperature difference 1500°C. No obvious cracks for MgAlON-15vol%BN composite were found in the same condition.

REFERENCES

- Willems, H. X., With, G. D. & Metsellar, R. (1993). Thermodynamics of AlON III: Stabilization of AlON with MgO. *Journal of European Ceramic Society*, Vol. 12, pp. 43-49. [1]
- Bandyopadhyay, S., Rixecker, G., Aldinger, F. & Maiti, H. S. (2004). Effect of Controlling Parameters on the Reaction Sequence of Formation of Nitrogen-containing Magnesium Aluminate Spinel from MgO, Al₂O₃ and AlN. *J. Am. Ceram. Soc.*, Vol. 87(3), pp. 480-482. [2]
- Deng, C. J., Hong, Y. R., Zhong, X. C. & Sun, J. L. (2000). Slag Resistance of MgAlON Spinel. *Journal of University of Science and Technology Beijing*, Vol. 7(2), pp. 96-99. [3]
- Wang, X. T., Zhang, B. G., Wang, H. Z., Sun, J. L. & Hong, Y. R. (2004). Sintering Properties of MgAlON-Spinel Composite Refractories. *Refractories*, Vol. 38, pp. 22-25. [4]
- Coblentz, W. S., & Lewis, III.D. (1988). In situ Synthesis of B₂O₃ with AlN and /or Si₃N₄ to form BN-toughened Composites. *Journal of American Ceramic Society*, Vol. 71(12), pp. 1080-1085. [5]
- Hayama, S., Ozawa, M. & Suzuki, S. (1996). Thermal Shock Fracture Behavior and Fracture Energy of Sialon-BN Composites. *Journal of Ceramic Society Japan*, Vol. 104, pp. 828-831. [6]
- Zhang, Z. T., Li, W. C., Wang, X. D. & Seetharaman, S. (2007). Synthesis and Characterization of MgAlON-BN Composites. *International of Journal Materials Research*, Vol. 1, pp.98-107. [7]
- Zhang, Z. T., Li, W. C., Teng, L. D. & Seetharaman, S. (2007). Mechanical Properties and Microstructures of Hot-pressed MgAlON-BN Composites. *Journal of European Ceramic Society*, Vol. 27, pp. 319-327. [8]
- Zhang, Z. T., Matsushita, T., Li, W. C. & Seetharaman, S. (2006). Investigation of Wetting Characteristics of Liquid Iron on Dense MgAlON-based Ceramics by X-Ray Sessile Drop Technique. *Metallurgical and Materials Transaction B*, Vol. 37, pp. 421-429. [9]
- Zhang, Z. T., Li, W. C. & Seetharaman, S. (2006). Thermal Diffusivity/Conductivity of MgAlON-BN Composites. *Metallurgical and Materials Transaction B*, Vol. 37, pp. 615-621. [10]
- Hasselmann, D. P. H. (1969). Unified Theory of Thermal Shock Fracture Initiation and Crack Propagation in Brittle Ceramics. *Journal of American Ceramic Society*, Vol. 52, pp. 600-604. [11]
- Hasselmann, D. P. H. (1963). Elastic Energy at Failure and Surface Energy as Design Criteria for Thermal Shock. *Journal of American Ceramic Society*, Vol. 46, pp. 535-540. [12]
- Hasselmann, D. P. H. (1970). *Thermal Stress Resistance Parameters for Brittle Refractory Ceramics: A Compendium*. American Ceramic Society Bulletin, Vol. 49, pp. 1033-1037. [13]
- Hasselmann, D. P. H. (1969). Analysis of the Strain at Fracture of Brittle Solids with High Densities of Microcracks. *Journal of American Ceramic Society*, Vol. 52(8), pp. 458-459. [14]
- Cemail, A. & Warren, P. D. (2003). Thermal Shock Parameters [R, R'' and R'''] of Magnesia-spinel Composites. *Journal of European Ceramic Society*, Vol. 23, pp. 301-308. [15]

- Cemail, A., Warren, P. D. & Riley, F. L.** (2004). Fracture Behaviour of Magnesia and Magnesia-Spinel Composites before and after Thermal Shock. *Journal of European Ceramic Society*, Vol. 24, pp. 2407-2316. [16]
- Annual Book of ASTM Standards** (1991). *Standard Test Method for Flexural Strength of Advanced Ceramics at Ambient Temperature*. Vol. C1161-90, pp. 327. [17]
- Annual Book of ASTM Standards** (1988). *Standard Test Methods for Flexural Properties of Unreinforced and Reinforced Plastics and Electrical Insulating Materials*. Vol. D790M-86, pp. 290. [18]
- Davidge, R. W. & Tappin, G.** (1967). The Effective Surface Energy of Brittle Materials. *Journal of Materials Science*, Vol. 3, pp. 165-173. [19]
- Coppola, J. A., Hasselman, D. P. H., & Bradt, R. C.** (1972). *On the Measurement of the Work of Fracture of Refractories*. American Ceramic Society Bulletin, Vol. 17, pp. 578-582. [20]
- Jiao, S., Jenkins, M. L. & Davidge, R. W.** (1997). *Interfacial Fracture Energy-mechanical Behaviour Relationship in Al_2O_3/SiC and Al_2O_3/TiN Nanocomposites*. Acta Materials, Vol. 45, pp. 149-156. [21]
- Selsing, J.** (1961). Internal Stresses in Ceramics. *Journal of American Ceramic Society*, Vol. 44(8), pp. 1419-1422. [22]

